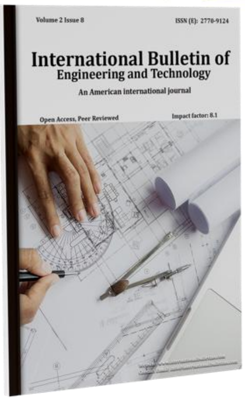

STABILITY FACTORS IN GAS METER VERIFICATION LABORATORIES: MATHEMATICAL MODELING AND ERROR CONTRIBUTION ASSESSMENT

Bekmurotov Chori Abdullayevich [1]
Associate Professor
Avezov Nodirbek Egambergonovich [1]
Inagamdjanov Doniyor Tuxtamuratovich [2]
Usmonov Hamzaali Qambarali ugli [2]
[1] Tashkent State Technical University named after Islam Karimov, Associate Professor of the Department of Metrology, Technical Regulation, Standardization and Certification, Doctor of Philosophy (PhD) in Technical Sciences.
[2] Uzbekistan National Metrology Institute, State Institution — Specialist, Independent Researcher.
https://doi.org/10.5281/zenodo.18539039

Abstract. Instability in verification facilities used for gas meter calibration arises from multiple physical and metrological factors, including pressure and temperature fluctuations, flow pulsations, gas compressibility and composition changes, hydraulic regime variations in pipelines, sensor drift, regulator dynamics, and reference channel uncertainties.

This paper proposes a **dynamic–static mathematical model** of a verification facility, decomposes instability sources into additive and multiplicative error components, and evaluates their contribution to the overall verification error variance. Sensitivity coefficients and Monte Carlo simulation are used to construct the uncertainty budget.

Keywords: gas meter, verification facility, instability, flow pulsation, measurement error, compressibility factor, Monte Carlo simulation.

Introduction. Operation of verification facilities for flow-measurement instruments and gas metering stations at gas-pumping compressor stations shows that the required level of metrological performance is not always achieved. In many cases, this is caused by non-uniform supply of the measured medium to metering instruments or to the working sections used for testing and calibration, as well as by uneven flow distribution among individual elements of the facility.

Numerous theoretical and experimental studies demonstrate that, under isothermal flow conditions in pressure pipelines, the velocity distribution across the pipe cross-section does not directly depend on the cross-sectional area, flow velocity, or physical properties of the transported medium. Instead, it is governed by dimensionless parameter complexes expressed through similarity criteria. Consequently, results obtained on one facility may be transferred to another, provided that hydrodynamic similarity conditions are satisfied.

However, in practice, verification facilities commissioned with identical capacity and equipped with similar instruments and equipment often exhibit different metrological characteristics. The primary reasons for such discrepancies lie in the structural features of individual installations, which promote flow separation from the surfaces of installation components, as well as external flow pulsations generated by equipment responsible for creating the flow. These effects result in flow non-uniformity and additional pulsations within the measurement channels of the facilities.

Separated flows constitute a complex area of fluid and gas mechanics. They are characterized by large pressure gradients, curvature of streamlines, and high levels of turbulent velocity fluctuations. Under such conditions, local reversal of the velocity vector may occur. It should be noted that the influence of separated flows on flow characteristics within verification facilities remains insufficiently studied.

In addition, coherent structures may develop within the flow, representing large-scale periodic vortex formations arising from instabilities in shear layers that evolve and interact against a background of small-scale turbulence [2]. The longitudinal dimensions of these structures are comparable to the transverse size of the channel, making their influence on measurement processes significant.

Flow separation typically occurs when the flow turns, during sudden channel expansions, in diffusers with large opening angles, in tees, and in other pipeline elements. Depending on installation design, one or several zones of flow separation and subsequent reattachment may occur. The locations of separation and reattachment points are generally not known in advance. In practice, the separation or reattachment point is defined as the coordinate where the time-averaged wall shear stress becomes zero.

In curved channels, which are widely used in verification facilities, centrifugal forces arising during flow turning cause redistribution of pressure and velocity. Static pressure increases in the direction away from the center of curvature, resulting in reduced velocity in that region. Conversely, pressure decreases toward the center of curvature, increasing velocity and potentially leading to flow separation from the channel walls. For a bend angle of approximately 90° with a small curvature radius, the vortex zone width may reach up to half of the channel cross-section, while its length typically extends to about three to four pipe diameters. Rounding the edges of bends significantly mitigates flow separation and improves velocity distribution. The larger the bend radius, the lower the flow non-uniformity and the shorter the downstream section required for velocity profile recovery.

In addition, instability in verification facilities used for the calibration of gas meters arises under the influence of a number of physical and metrological factors, including pressure and temperature fluctuations, flow pulsations, variations in gas compressibility and composition, changes in hydraulic flow regimes within test pipelines, sensor drift, regulator dynamics, and uncertainty in the reference measurement channel.

This paper proposes a dynamic–static mathematical model of the verification facility, in which instability sources are decomposed into additive and multiplicative error components, and their contributions to the overall variance of verification error are evaluated. Based on the model, sensitivity coefficients and Monte Carlo simulation are employed to construct the measurement uncertainty budget.

General measurement equation for verification. During verification, the flow rate measured by the device under test (DUT), Q_d, is compared with the flow rate obtained from the reference channel (REF), Q_r.

Relative verification error is defined as (1):

$$\delta = \frac{Q_d - Q_r}{Q_r}. \tag{1}$$

IBET | Volume 6, Issue 02, February

Reference flow is often converted to standard conditions using pressure, temperature, and compressibility parameters:

$$Q_r = Q_{line} \cdot K_{conv}, \qquad K_{conv} = \frac{P}{P_s} \cdot \frac{T_s}{T} \cdot \frac{Z_s}{Z}. \tag{2}$$

Where:

– Q_{line} is the measured flow under line conditions,
– P,T, Z are line pressure, temperature, and compressibility factor,
– Ps,Ts, Zs correspond to standard conditions.

This,

$$\delta = \frac{Q_d - Q_{line} K_{conv}}{Q_{line} K_{conv}}. \tag{3}$$

Classification of Instability Sources

Instability sources are grouped as follows:

– Thermodynamic factors: Fluctuations in P(t), T(t), and Z(t) due to composition or humidity changes.

– Hydrodynamic factors: Flow pulsations, turbulence regime changes, regulator or valve dynamics.

– Instrumental factors: Sensor drift, calibration coefficient variations, signal noise.

– Methodological factors: Time synchronization errors, averaging algorithms, and measurement interval selection.

Dynamic mathematical model

1 Flow Model

Flow is represented as an average value plus pulsation (4):

$$Q_{line}(t) = \bar{Q} + \tilde{Q}(t), \tag{4}$$

where Õ(t) is a random or periodic component. A possible representation is AR:

$$\tilde{Q}_k = \varphi \tilde{Q}_{k-1} + \varepsilon_k, \qquad \varepsilon_k \sim \mathcal{N}(0, \sigma_Q^2). \tag{5}$$

2 Pressure and Temperature Variations

Pressure and temperature are expressed as (6):

$$P(t) = \bar{P} + \tilde{P}(t), \qquad T(t) = \bar{T} + \tilde{T}(t), \tag{6}$$

where fluctuations include drift and noise (7):

$$\tilde{P}(t) = d_P t + n_P(t), \qquad \tilde{T}(t) = d_T t + n_T(t). \tag{7}$$

3 Sensor Errors and Drift

Measured values are:

$$P_m(t) = P(t)(1+\alpha_P) + b_P(t) + \eta_P(t),$$
$$T_m(t) = T(t)(1+\alpha_T) + b_T(t) + \eta_T(t), \tag{8}$$

Where α represents scale error, b(t) drift, and η(t) random noise.

4 Conversion Coefficient
The conversion coefficient becomes time-dependent:

$$K_{conv}(t) = \frac{P_m(t)}{P_s} \cdot \frac{T_s}{T_m(t)} \cdot \frac{Z_s}{Z(t)}. \tag{9}$$

This,

$$Q_r(t) = Q_{line}(t)\, K_{conv}(t). \tag{10}$$

Influence of averaging interval
Measured values are averaged over interval τ:

$$\hat{Q}_r = \frac{1}{\tau}\int_{t_0}^{t_0+\tau} Q_r(t)\,dt, \quad \hat{Q}_d = \frac{1}{\tau}\int_{t_0}^{t_0+\tau} Q_d(t)\,dt. \tag{11}$$

A longer interval reduces high-frequency pulsations but may accumulate drift errors. Therefore, an optimal averaging interval exists.

Analytical Estimation Using Sensitivity Method
For small deviations:

$$\delta \approx c_Q\,\Delta Q_{line} + c_P\,\Delta P_m + c_T\,\Delta T_m + c_Z\,\Delta Z + c_d. \tag{12}$$

If REF channel errors dominate:

$$\delta \approx -\frac{\Delta Q_r}{\bar{Q}_r}. \tag{13}$$

$$\frac{\Delta Q_r}{\bar{Q}_r} \approx \frac{\Delta Q_{line}}{\bar{Q}_{line}} + \frac{\Delta P_m}{\bar{P}} - \frac{\Delta T_m}{\bar{T}} - \frac{\Delta Z}{\bar{Z}}. \tag{14}$$

Variance becomes:

$$\sigma_\delta^2 \approx \sigma_Q^2 + \sigma_P^2 + \sigma_T^2 + \sigma_Z^2. \tag{15}$$

With correlated variables:

$$\sigma_{\delta}^{2} \approx \sum_{i} \sigma_{i}^{2} + 2 \sum_{i<j} \mathrm{Cov}(x_i, x_j). \tag{16}$$

EXAMPLE:

1) Nominal Operating Conditions

The simulation used the following nominal values:

– Line flow rate: $\mathbf{Q_{line0} = 100}$ (arbitrary units)
– Pressure: $\mathbf{P_0 = 20}$ **bar**
– Temperature: $\mathbf{T_0 = 293.15}$ **K**
– Compressibility factor: $\mathbf{Z_0 = 0.90}$
– Standard conditions: **Ps = 1.01325 bar**, **Ts = 293.15 K**, **Zs = 1.0**

$$Q_{std} = Q_{line} \cdot \frac{P}{P_s} \cdot \frac{T_s}{T} \cdot \frac{Z_s}{Z}$$

Flow conversion to standard conditions:

Calculation at nominal point

Since $T_s = T_0$,

$$Q_{std,0} = 100 \cdot \frac{20}{1.01325} \cdot \frac{1}{0.90} \approx 2193.16$$

Thus, nominal standard flow is approximately **2193.16 units.**

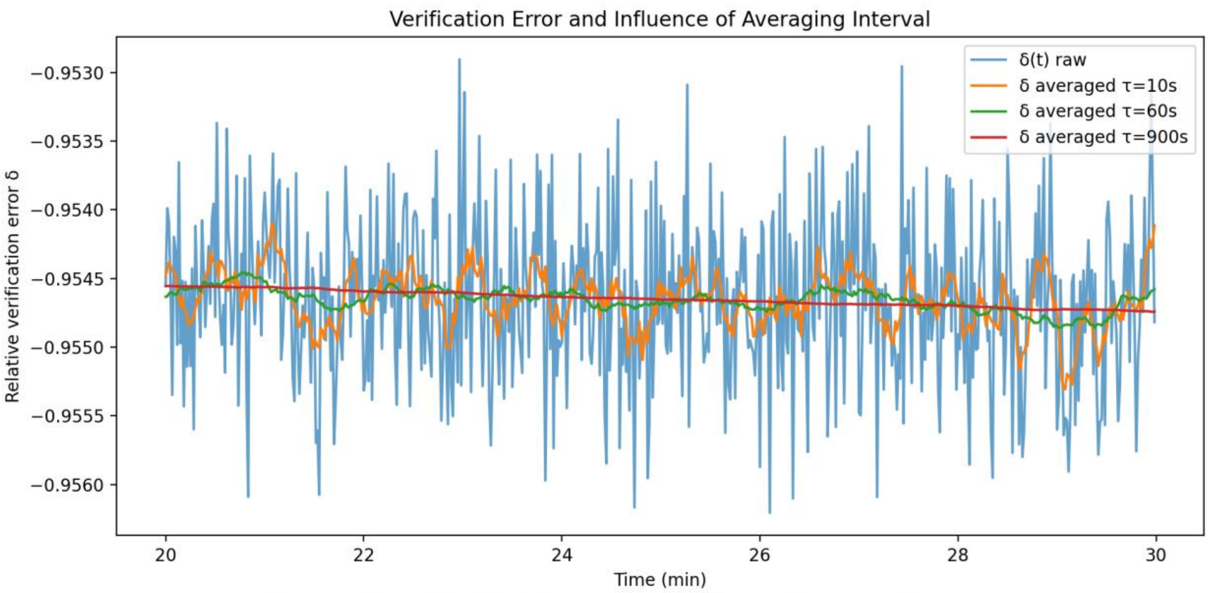

Figure 1— Verification error δ (t) and averaging

2) Influence of P, T, Z Variations (Numerical Example)

Assume at some moment:

– Pressure: **P = 20.05 bar**
– Temperature: **T = 292.95 K**
– Compressibility: **Z = 0.902**

IBET | Volume 6, Issue 02, February

Then,

$$Q_{std} = 100 \cdot \frac{20.05}{1.01325} \cdot \frac{293.15}{292.95} \cdot \frac{1}{0.902} \approx 2195.27$$

Difference from nominal:

– Absolute change:

$$\Delta Q_{std} \approx 2.11$$

Relative change:

$$\frac{2.11}{2193.16} \approx 0.096\%$$

Sensitivity-based quick estimation
For small deviations,

$$\frac{\Delta Q}{Q} \approx \frac{\Delta P}{P} - \frac{\Delta T}{T} - \frac{\Delta Z}{Z}$$

Numerically:
- $\Delta P/P = 0.25\%$
- $-\Delta T/T = +0.068\%$
- $-\Delta Z/Z = -0.222\%$

Total ≈ **0.096%**, matching the full calculation.

3) Sensor Errors: Scale, Drift, Noise

Table-1. Simulation parameters for REF sensors.

Sensor	Scale error	Drift rate	Noise level
Flow Q	+0.4%	2×10^{-4} /s	±0.8
Pressure P	−0.2%	-2×10^{-5} /s	±0.06 bar
Temperature T	+0.1%	4×10^{-4} /s	±0.35 K
Z factor	+0.2%	0	±0.0005

After **1 hour (3600 s)**:
– Flow drift: 0.72 units
– Pressure drift: −0.072 bar
– Temperature drift: +1.44 K

Measured values become approximately:

– $Q_{ref} \approx 101.12 \pm 0.8$
– $P \approx 19.888 \pm 0.06$ bar
– $T \approx 294.883 \pm 0.35$ K
– $Z \approx 0.9018 \pm 0.0005$

Converted standard flow becomes approximately: $Q_{ref,std} \approx 2187.78$

4) Verification Error Example

$$\delta = \frac{Q_{DUT} - Q_{REF}}{Q_{REF}}$$

Verification error:
Example:
– Reference flow: 2187.78
– DUT flow: 2201.9

$\delta = 0.645\ \%$

Table-2

τ (s)	Var(δ)	Std(δ)
1	9.26×10^{-7}	0.096%
10	6.17×10^{-7}	0.078%
60	5.79×10^{-7}	0.076%
300	5.34×10^{-7}	0.073%
600	4.85×10^{-7}	0.070%
900	**4.41×10^{-7}**	**0.066%**

Minimum variance occurs at **τ ≈ 900 s**.
Averaging reduces pulsations but too long averaging may accumulate drift.

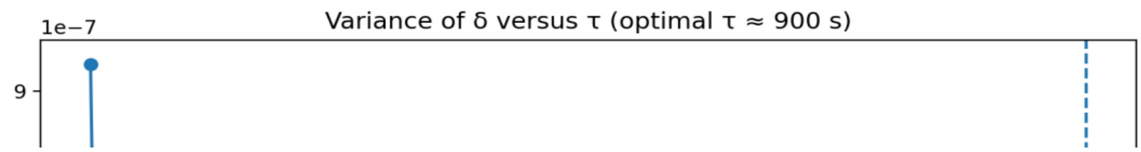

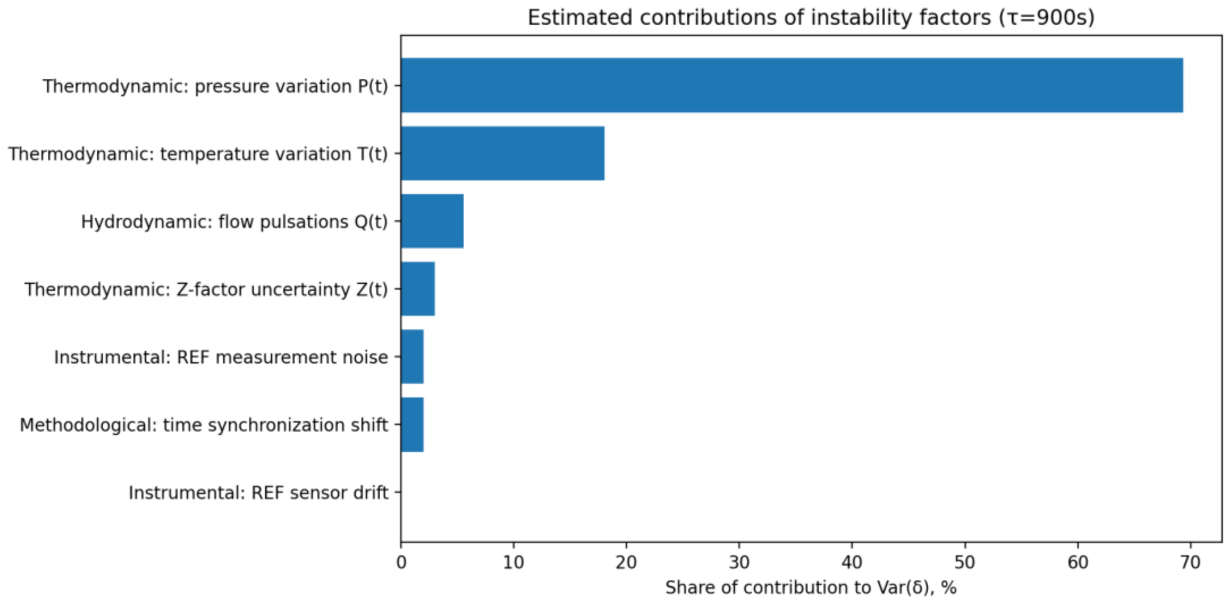

Figure 4 — Contributions of instability factors

6) Contribution of Instability Factors

Table-3. Variance contribution results.

Factor	Contribution
Pressure instability	69.3%
Temperature instability	18.1%
Flow pulsations	5.6%
Z uncertainty	3.0%
REF noise	2.0%
Time synchronization error	2.0%
Sensor drift	~0% (in this scenario)

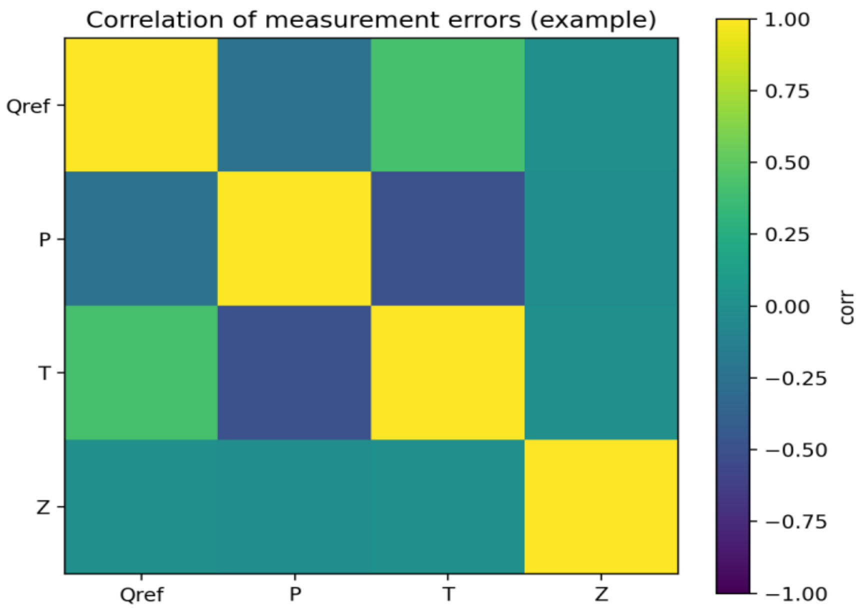

Figure 5 — Correlation of measurement errors

Monte carlo simulation procedure

Simulation steps:

1. Set nominal conditions $\bar{Q}, \bar{P}, \bar{T}, \bar{Z}$.
2. Generate random processes for flow, pressure, and temperature.
3. Add sensor errors and drift.
4. Compute K*conv*(t) and Q_r(t).
5. Average over interval τ.
6. Calculate error δ and repeat simulations.
7. Estimate mean error, standard deviation, and contribution of each factor.

Interpretation of typical results

Simulation usually shows:

– Increasing averaging interval reduces pulsation effects.
– Excessive averaging increases drift influence.
– Temperature channel instability strongly affects conversion accuracy.
– Compressibility factor errors are critical at high pressure.
– Correlations between flow and pressure may increase or decrease total uncertainty.

Engineering recommendations

To reduce instability:

1. Stabilize flow and reduce pulsations.
2. Improve thermal insulation and temperature measurement placement.
3. Ensure synchronized measurements.
4. Optimize averaging algorithms.
5. Consider gas composition when calculating compressibility.
6. Maintain uncertainty budgets for all channels.

Conclusion

The proposed mathematical model describes instability through flow, pressure, temperature, compressibility, and sensor drift parameters. Sensitivity and Monte Carlo analyses help identify dominant error sources and optimize verification conditions, averaging intervals, and equipment specifications

Literature:

1.Idelchik, I. E. Aerodynamics of Technological Apparatus. Moscow: Mashinostroenie Publishers, 1983, 351 p.

2.Ginevskiy, A. S., Vlasov, E. V., Karavosov, R. K. Acoustic Control of Turbulent Jets. Moscow: FIZMATLIT, 2001, 240 p. ISBN 5-9221-0161-7.

3.Mikheev, N. I., Molochnikov, V. M., Davletshin, I. A., et al. Hydrodynamic and heat transfer processes in pulsating flow. In: Proceedings of the VI School-Seminar on Problems of Heat and Mass Transfer and Hydrodynamics in Power Engineering. Kazan, 2008, pp. 48–76.

4.Gündogdu, M. Y., Carpinlioglu, M. O. Present State of the Art on Pulsatile Flow Theory (Part 1: Laminar and Transitional Flow Regimes). Journal of the Japan Society of Mechanical Engineers, Series B, 1999, Vol. 42, No. 3, pp. 384–397.

5.Gündogdu, M. Y., Carpinlioglu, M. O. Present State of the Art on Pulsatile Flow Theory (Part 2: Laminar and Transitional Flow Regimes). Journal of the Japan Society of Mechanical Engineers, Series B, 1999, Vol. 42, No. 3, pp. 398–410.

6.Alemasov, V. E., Glebov, G. A., Kozlov, A. P. Thermoanemometric Methods for Studying Separated Flows. Kazan: Kazan Branch of the USSR Academy of Sciences, 1989, 178 p.